Supplementary Material

Efficient light-driven fuel cell with simultaneous degradation of pollutants on TiO_2 photoanode and production of H_2O_2 on gas diffusion electrode (GDE) cathode

*Tian Wang[a], Fei Ye[b], Shuai Wu[a], Shuo Chen[a], Hongtao Yu[a], Xie Quan[a,]**

[a]Key Laboratory of Industrial Ecology and Environmental Engineering (Ministry of Education, China), School of Environmental Science and Technology, Dalian University of Technology, Dalian 116024, China

[b]School of Environmental and Chemical Engineering, Yanshan University, Qinhuangdao 066004, China

*Corresponding author.

Email address: quanxie@dlut.edu.cn

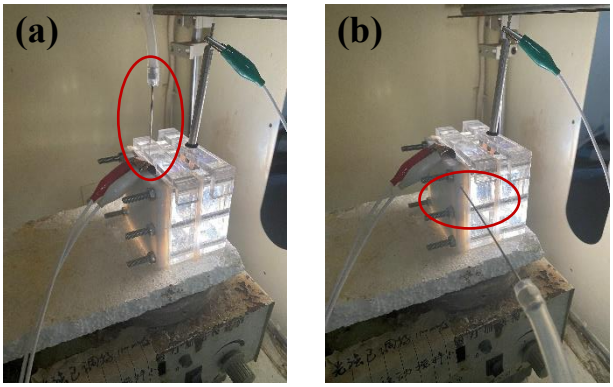

Figure S1. The real images of (a) normal aeration mode and (b) gas diffusion aeration mode.

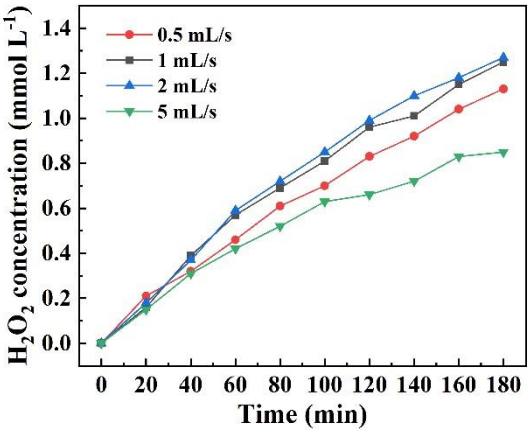

Figure S2. The effect of O_2 flow rate on H_2O_2 generation.

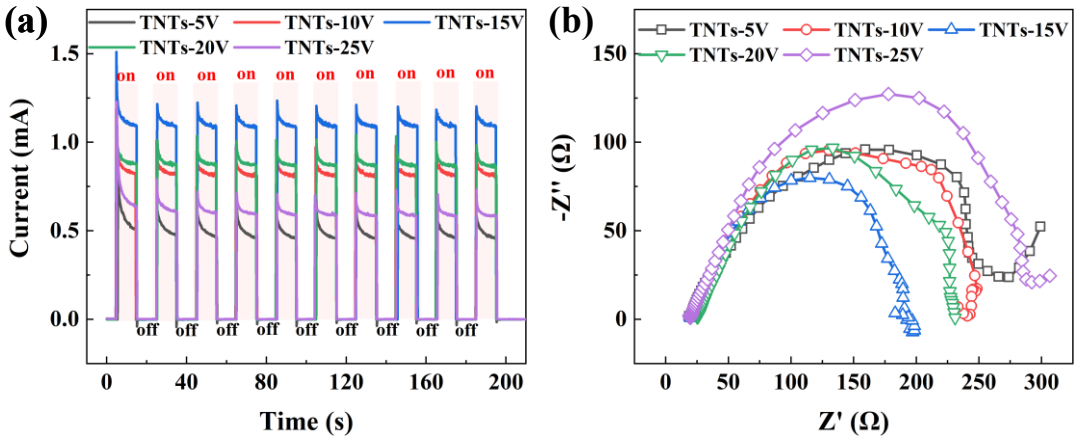

Figure S3. (a) Photocurrent-time curves and (b) Nyquist plots of TNTs-x V (x= 5, 10, 15, 20 and 25). Experiment conditions: 0.05 M Na_2SO_4, 0 V bias potential, simulated solar light (λ: 320-780 nm) illumination.

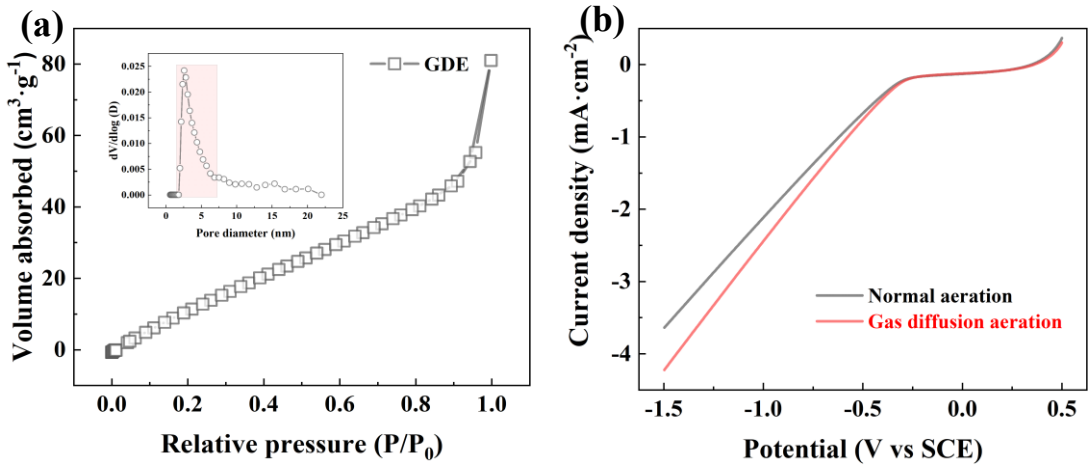

Figure S4. (a) N_2 adsorption-desorption isotherms and pore distribution (inset) of GDE and (b) LSV of GDE (black line: normal aeration, red line: gas diffusion).

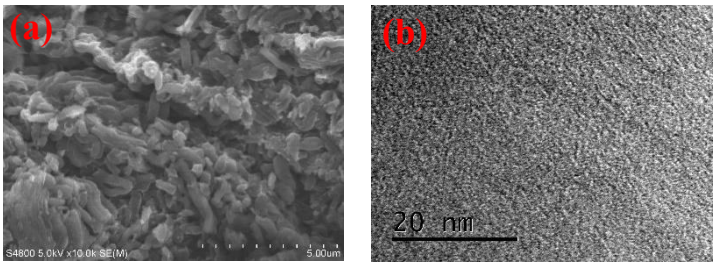

Figure S5. (a) SEM and (b) TEM images of the CMK-3.

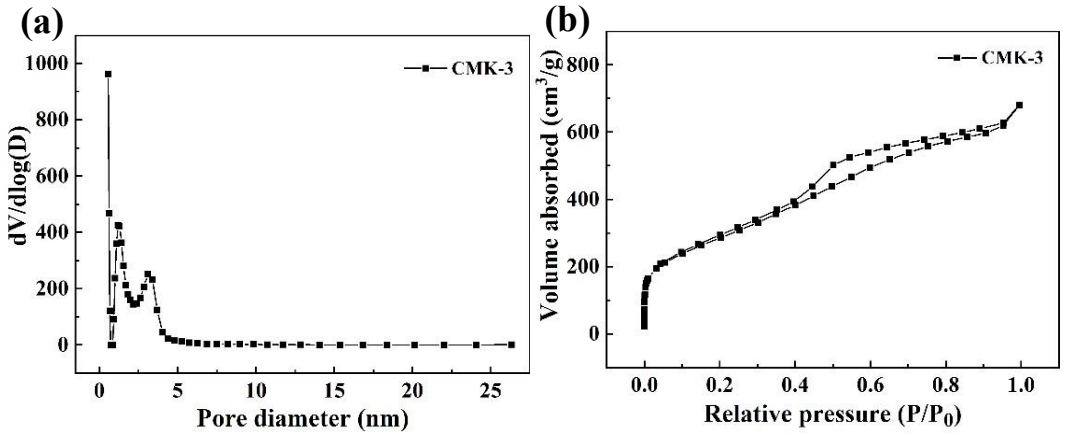

Figure S6. (a) N_2 adsorption-desorption isotherms and (b) pore distribution of the CMK-3.

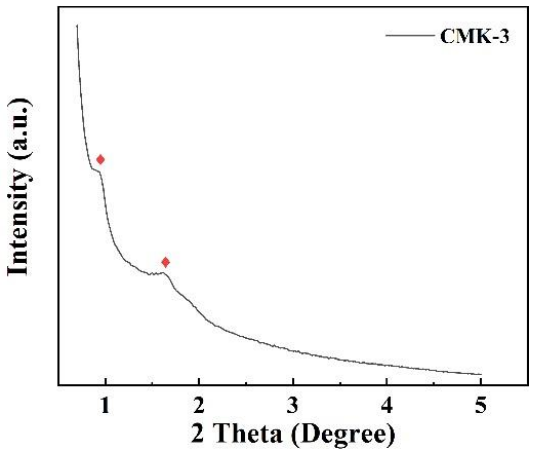

Figure S7. XRD pattern of the CMK-3.

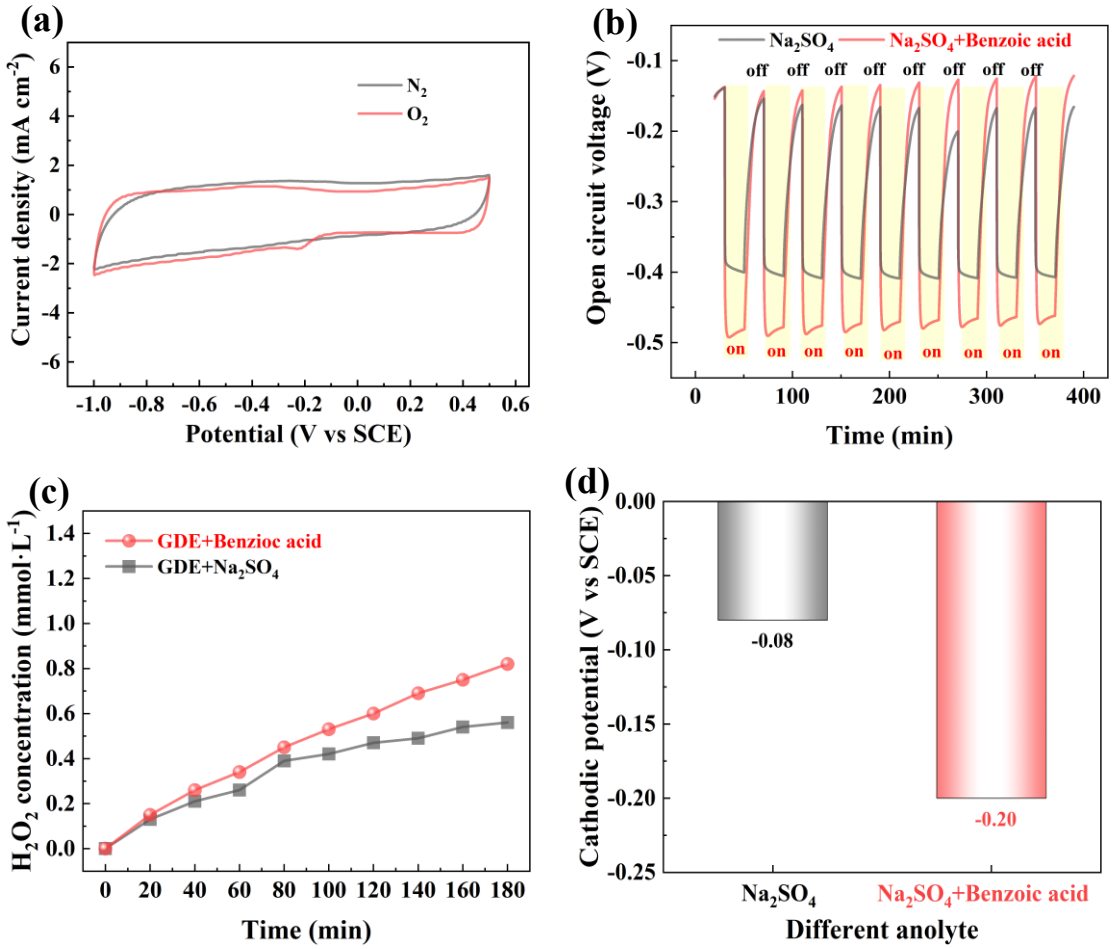

Figure S8. (a) CV plots of CMK-3 (black line: N_2 saturated, red line: N_2 saturated) and the influence of benzoic acid on (b) Open circuit voltage, (c) H_2O_2 production and (d) Cathodic potential of GDE-TiO_2 system.

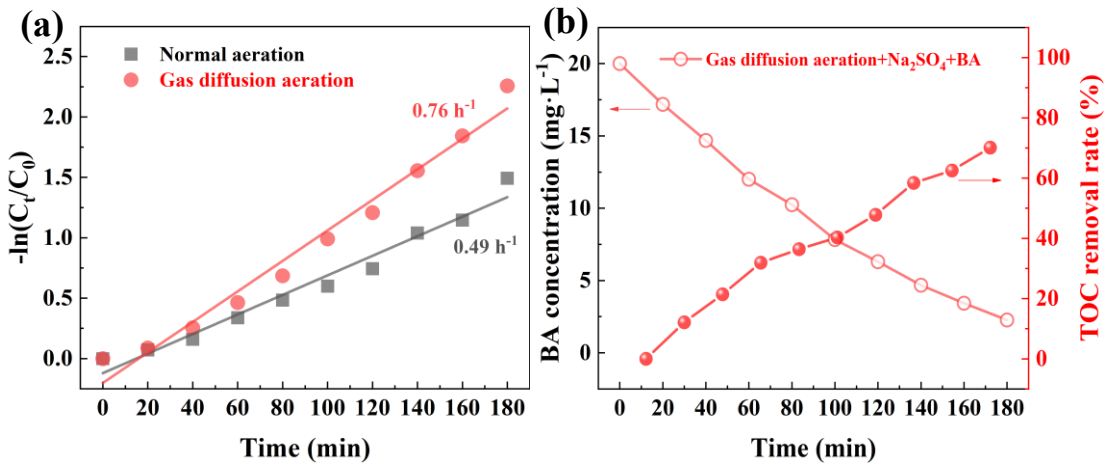

Figure S9. (a) The degradation kinetics of Phenol under different aeration mode (red line: gas diffusion aeration, black line: normal), (b) The degradation and mineralization plots of Benzoic Acid in the GDE-TiO_2 system.

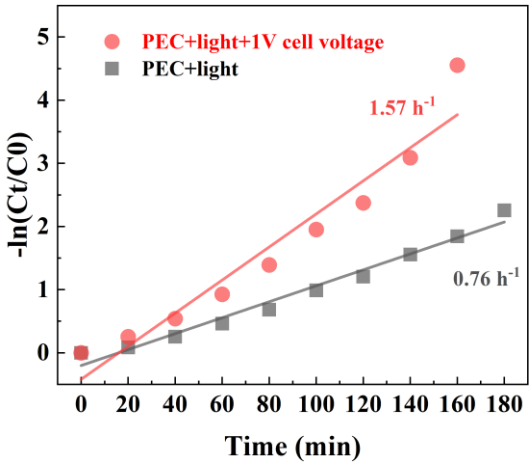

Figure S10. The degradation kinetics of Phenol in the GDE-TiO_2 system under different cell voltages (red line: PEC + light + 1 V cell voltage, black line: PEC + light).

Table S1. Summary of performance comparison of similar PEC systems.

	PEC system	External voltage	Yield of H_2O_2 normalized by cathode areas		Faraday efficiency of H_2O_2	Reference
System without external voltage	Anode: WO_3 Cathode: FPC	Three-electrode system 0V anodic bias potential	10 μmol/L/h/cm^2	0.2 μmol/h/cm^2	66%	S1
	Anode: P-Mo-$BiVO_4$ Cathode: AQ-CNT/C	Three-electrode system 0V anodic bias potential		9.6 μmol/h/cm^2 (A net yield of anode and cathode)	Photoanodic: 40%-50% Cathodic: ~100%	S2
	Anode: WO_3/$BiVO_4$ Cathode: Pt	Three-electrode system 0 V anodic bias potential	~37.9 μmol/L/h/cm^2 (High concentration $KHCO_3$ solution of 2 M)	1.33 μmol/h/cm^2	~54%	S3
	Our work (light only)	Two-electrode system 0V cell voltage	34.7 μmol/L/h/cm^2	1.39 μmol/h/cm^2	70.9%	
System with external voltage	Anode: WO_3 Cathode: FPC	Three-electrode system 1V anodic bias potential	187.5 μmol/L/h/cm^2	3.75 μmol/h/cm^2	75%	S1
	Anode: P-Mo-$BiVO_4$ Cathode: AQ-CNT/C	Three-electrode system 1V anodic bias potential		39.6 μmol/h/cm^2	Photoanodic: ~43% Cathodic: ~100%	S2
	Anode:TO-TiO_2 Cathode: graphite sheet	Three-electrode system 10 mA constant current	184 μmol/L/h/cm^2	1.68 μmol/h/cm^2	~75%	S4
	Anode: WO_3/$BiVO_4$ Cathode: Pt	Three-electrode system 1 mA constant current	~42.4 μmol/L/h/cm^2 (0.5 M $KHCO_3$ solution)	~1.48 μmol/h/cm^2		S3
	Anode: WO_3 Cathode: CF/DPA	Three-electrode system -0.5 V cathodic bias potential	108 μmol/L/h/cm^2			S5
	Anode: DSA/IrO_2 Cathode: g-C_3N_4	Three-electrode system -0.7 V cathodic bias potential	185.2 μmol/L/h/cm^2	18.5 μmol/h/cm^2		S6
	Anode: WO_3 Cathode: mesoporous carbon	Three-electrode system 1 V anodic bias potential	132 μmol/L/h/cm^2	19.8 μmol/h/cm^2	73%	S7
	Anode: α-Fe_2O_3 nanorods Cathode: GDE	Three-electrode system 0.5 V anodic bias potential	58.8 μmol/L/h/cm^2		32.5%	S8
	Our work (light+1 V voltage)	Two-electrode system 1V cell voltage	266 μmol/L/h/cm^2	10.6 μmol/h/cm^2	73.6%	

S1. Ye, F.; Wang, T.; Quan, X.; Yu, H.; Chen, S., Constructing Efficient WO_3-FPC System for Photoelectrochemical H_2O_2 Production and Organic Pollutants Degradation. *Chem. Eng. J.* **2020,** *389*, 123427.

S2. Jeon, T. H.; Kim, H.; Kim, H.-i.; Choi, W., Highly Durable Photoelectrochemical H_2O_2 Production via Dual Photoanode and Cathode Processes under Solar Simulating and External Bias-Free Conditions. *Energy Environ. Sci.* **2020,** *13* (6), 1730-1742.

S3. Fuku, K.; Sayama, K., Efficient Oxidative Hydrogen Peroxide Production and Accumulation in Photoelectrochemical Water Splitting Using a Tungsten Trioxide/Bismuth Vanadate Photoanode. *Chem. Commun.* **2016**, *52* (31), 5406.

S4. Leng, W. H.; Zhu, W. C.; Ni, J.; Zhang, Z.; Zhang, J. Q.; Cao, C. N., Photoelectrocatalytic Destruction of Organics Using TiO_2 as Photoanode with Simultaneous Production of H_2O_2 at the Cathode. *Appl. Catal. A-Gen.* **2006**, *300* (1), 24-35.

S5. Xiao, K.; Liang, H.; Chen, S.; Yang, B.; Zhang, J.; Li, J., Enhanced Photoelectrocatalytic Degradation of Bisphenol A and Simultaneous Production of Hydrogen Peroxide in Saline Wastewater Treatment. *Chemosphere* **2019**, *222*, 141-148.

S6. Yu, F.; Wang, Y.; Ma, H.; Dong, G., Enhancing the Yield of Hydrogen Peroxide and Phenol Degradation via a Synergistic Effect of Photoelectrocatalysis Using a g-C_3N_4/ACF Electrode. *Int. J. Hydrog. Energy*. **2018**, *43* (42), 19500-19509.

S7. Papagiannis, I.; Doukas, E.; Kalarakis, A.; Avgouropoulos, G.; Lianos, P., Photoelectrocatalytic H_2 and H_2O_2 Production Using Visible-Light-Absorbing Photoanodes. *Catalysts* **2019,** *9* (3), 243.

S8. Mei, X.; Bai, J.; Chen, S.; Zhou, M.; Jiang, P.; Zhou, C.; Fang, F.; Zhang, Y.; Li, J.; Long, M.;

Zhou, B., Efficient SO_2 Removal and Highly Synergistic H_2O_2 Production Based on a Novel Dual-Function Photoelectrocatalytic System. *Environ. Sci. Technol.* **2020,** *54* (18), 11515-11525.

The detailed calculation of energy consumption

The calculation method [S9] of energy consumption is as follows:

$$P=\frac{U\times I\times t}{3600}=\frac{U\times Q}{3600}$$

In this equation, P is the total power (W), U is the potential difference between photoanode and cathode (V), I is the current (A), t is the reaction time (s), Q is the quantity of charge transferred (C).

In experimental operation, U is obtained by the open circuit voltage test, Q is acquired directly from electrochemical workstation. When testing the integrated system, the TiO_2 was used as photoanode coupled with the GDE as both cathode and reference electrode. Except for the potential difference between the TiO_2 and GDE obtained by the open circuit potential test, the cathodic and anodic potential were obtained by using an additional multimeter. Considering the anodic half reaction (Pt sheet as the counter electrode and SCE as reference electrode) for phenol degradation, a stable potential measured previously in the integrated system was applied to TiO_2 by electrochemical workstation. It is similar to dealing with the cathodic half reaction.

S9. Guo, C.; He, P.; Cui, R.; Shen, Q.; Yang, N.; Zhao, G., Electrochemical CO_2 Reduction Using Electrons Generated from Photoelectrocatalytic Phenol Oxidation. *Adv. Energy Mater.* **2019**, *9* (18), 1900364.